

# A novel method for estimating SBRT delivered dose with beam's-eye-view images

Ross I. Berbeco<sup>a)</sup> and Fred Hacker

*Department of Radiation Oncology, Brigham and Women's Hospital, Dana-Farber Cancer Institute and Harvard Medical School, Boston, Massachusetts 02115*

Chris Zatwarnicki

*Department of Radiation Oncology, Brigham and Women's Hospital, Dana-Farber Cancer Institute and Harvard Medical School, Boston, Massachusetts 02115 and Department of Radiation Oncology, Duke University Medical Center, Durham, North Carolina 27710*

Sang-June Park, Dan Ionascu, Desmond O'Farrell, and Harvey J. Mamon

*Department of Radiation Oncology, Brigham and Women's Hospital, Dana-Farber Cancer Institute and Harvard Medical School, Boston, Massachusetts 02115*

(Received 22 January 2008; revised 7 May 2008; accepted for publication 8 May 2008; published 19 June 2008)

Stereotactic body radiation therapy is predicated on a high degree of targeting accuracy. However, inaccurate patient setup as well as intra-fractional motion can hinder the delivery of high doses preferentially to the target. To ensure that the coverage delivered to the patient is as planned, an image-guided verification system has been created to estimate the delivered dose retrospectively. This will not only aid the assessment of treatment techniques, but will also allow for more accurate dose response analysis. Patients with limited hepatic metastases from solid tumors were treated with SBRT. Implanted gold markers were used as target surrogates and a body frame and compression plate provided stereotactic localization and target immobilization, respectively. During treatment, an electronic portal imaging device (EPID), operating in *cine* mode, collected the exit dose. The sequences of images for each field were processed off-line using in-house software for registration and seed localization. The beam's-eye-view seed positions in the treatment images were compared to those in the DRR's to determine the target shifts in the imaging plane. These target shifts were then imported into the treatment planning software. Each original field was multiplied by the number of images taken during treatment. The calculated shift from each image was then applied to each of the new subfields. Summing all of these subfields together gives the dose distribution that was actually delivered to the patient. The dose-volume histograms for the planned and delivered distributions for four patients' complete treatments are shown. For two of the patients, underdosing due to a setup error or intra-fractional drift was not wholly resolved by subsequent fractions. For one of these patients two alternative corrective strategies have been applied, retrospectively, and the prescribed target coverage recovered for both. The delivered dose can be estimated using the information contained in cine EPID images acquired during irradiation. Calculating the dose actually delivered to the target will allow us to assess treatment procedures as well as more accurately report clinical results. © 2008 American Association of Physicists in Medicine.

[DOI: [10.1118/1.2938514](https://doi.org/10.1118/1.2938514)]

Key words: SBRT, EPID, delivered dose, liver, radiotherapy

## I. INTRODUCTION

Currently, clinical studies in radiation therapy tend to report patient outcomes as a function of *planned dose*. As *in vivo* dosimetry is not readily available, investigators tend to work under the assumption that the planned dose distribution is what is actually delivered to the patient. This assumption is implicit in clinical evaluations of treatment response. In dose escalation studies, for example, the patient response is given as a function of the prescribed or planned dose, with no effort to determine the dose that was actually *delivered* to the target. This can cause inconsistencies among data sets that are collected at different institutions or even within the same institution if significant variation in target localization occurs. It would be clinically useful to have a method for cal-

culating the distribution of radiation dose that is delivered to the target. This information could be used for dose response studies, as the basis for additional courses of radiotherapy treatment, and for quality assurance purposes. We are proposing a method for estimating the delivered treatment dose in three dimensions without disturbing the treatment itself in any way or adding any risk to the patient. A viable technique would allow the reporting of any clinical endpoints as a function of *delivered dose*, thus permitting the real dose-response relationship to be investigated.

Several other methods have been proposed for calculating the dose delivered to patients. Scarantino *et al.* have reported on an implantable dosimeter for measuring dose to a point within the patient.<sup>1</sup> This is an excellent method for verifying

TABLE I. Treatment parameters for the patients studied.

Patient	Prescription (Gy)	Fractions	Beams	Gantry (couch) angles (IEC)	Images/fraction
1	30	3	8	40 (0), 315 (0), 270 (0), 220 (0), 0 (90), 25 (90), 270 (345), 270 (15)	170
2	25	5	9 Co-planar	45, 15, 345, 315, 285, 255, 225, 195, 165	80
3	45	5	8 Co-planar	290, 270, 250, 230, 180, 135, 90, 75	180
4	30	3	6	20 (90), 315 (0), 225 (0), 170 (90), 270 (15), 90 (350)	190

the dose delivered to a single point, perhaps near an organ at risk. Several authors have proposed using an on-treatment cone-beam CT (CBCT) to calculate delivered dose.<sup>2</sup> Although the imaging does provide volumetric information at the beginning of the fraction, it cannot account for internal changes that may occur while the treatment beam is on. McDermott *et al.* have proposed using a combination of portal imaging and CBCT to calculate the delivered dose in the case of rectal cancer patients.<sup>3</sup> This may work with static anatomy, but problems will arise when motion is introduced, as is often the case in the abdomen and thorax. Ultimately, the ideal imaging modality would provide volumetric information during delivery. A few investigators have proposed the use of magnetic resonance imaging during either LINAC or Cobalt based radiotherapy delivery, but these are still in the early stages of development.<sup>4-6</sup> Litzenberg *et al.* have proposed calculating delivered dose using implanted RF transponders as a surrogate for internal anatomy.<sup>7</sup> However, these devices have only been approved for use in the prostate. Our method uses gold fiducial markers, which can be implanted in most treatment sites. These markers show up well in x-ray imaging, even in the MV energy range, which is the modality used for this study.

Many new linear accelerators (LINACS) come equipped with an electronic portal-imaging device (EPID) that is generally used for acquiring portal images with the megavoltage (MV) beam prior to treatment. Normally, after the patient setup is complete, the EPID is retracted back into the linac base for the duration of the therapeutic irradiation. We are proposing to leave the EPID in its extended, acquisition position and collect the exit radiation during conformal (non-IMRT) radiotherapy. With the EPID set to acquire in *cine* mode, it generates a sequence of beam's-eye-view (BEV) images similar to fluoroscopy, albeit at a lower frame rate. The beam's-eye view is the most important direction for MV x-ray treatment verification because the dose falloff in the degenerate direction (along the beam line) is much less than in the cross-plane directions. Important localization information is lost if the beam's-eye view is not used. Data are collected for each treatment beam. No time is added to the treatment and negligible additional dose is given to the patient.<sup>8</sup> This verification method was first implemented for respiratory-gated liver patients,<sup>9</sup> but we have since moved on to monitor continuous (nongated) treatments for liver and lung patients.

With the technique described above, it will be demonstrated that it is possible to calculate the delivered dose distribution while the patient still has fractions remaining. It may be advantageous to modify the treatment plan if the delivered distribution shows poor agreement with the prescription. Areas of undesired under-dosing (e.g., the target) could be replanned to regain the desired coverage, and areas of unanticipated over-dosing could be avoided to reduce the probability of harm to normal structures. We call this convergent radiation therapy (CRT): replanning between fractions, based on the delivered dose distribution, so that, as treatment progresses, the delivered dose coverage converges with the planned dose coverage. CRT differs from the concept of adaptive radiation therapy, as described by Yan *et al.*,<sup>10</sup> in that the delivered dose is used to modify the plan for future fractions. CRT becomes more important as the number of fractions is reduced; in a hypofractionated treatment there are fewer opportunities to "wash out" an aberration that might occur on a single day. It will be shown how the concept of CRT can be applied to a stereotactic body radiation therapy (SBRT) treatment that would otherwise not have achieved the desired dose coverage.

## II. MATERIALS AND METHODS

### II.A. Data acquisition

The data used in this study were acquired from four patients receiving SBRT treatment for liver metastases at the Brigham and Women's Hospital in Boston, MA. Table I includes the treatment parameters for the patients included in this study. Three radiopaque fiducial markers (gold "seeds") are implanted near the tumor prior to scanning. Simulation and treatment are performed with the patients in a stereotactic body frame and an abdominal compression plate to restrict liver motion due to respiration (Elekta Instruments, Stockholm, Sweden). Target residual motion is assessed with kV fluoroscopy. A subset of the patients underwent 4DPET/CT scans to further assess the residual motion; however no additional information was gleaned so the practice was ended. For treatment planning, the GTV is determined by the physician using CT and PET imaging. The GTV is expanded directly to the PTV by a patient-specific safety margin designed to include residual respiratory motion. Digitally reconstructed radiographs (DRRs), which include the

field aperture and implanted marker locations, are produced for each of the planned fields. During treatment, the EPID is left in its acquisition position and BEV *cine* images are collected for each treatment beam. For this study, a frame rate of 0.7 Hz was used. The planar *cine* EPID images show the collimator aperture and the implanted fiducials. The seed positions relative to the aperture can be evaluated qualitatively during treatment; but for quantitative analysis, the images must be exported off-line. After the application of a high-pass filter to improve the visibility of the seeds in the images, less than 1% of the images contained one or more seeds that were not visible due to poor contrast. A more thorough description of this process and the analysis of the EPID images can be found in a previous publication.<sup>11</sup>

## II.B. Three-dimensional dose estimation

A program has been written in IDL (Research Systems Inc.) that allows the user to move through the images and manually select the aperture and seed locations in each one. Originally these data were used to report the target location as a function of time for each beam and for multiple beams. To calculate the delivered dose distribution, the treatment seed positions are compared to the DRR seed positions. The relative shift of the target in the imaging plane is calculated for each of the treatment fields. This value is defined as the average difference of the seed positions in the EPID images relative to the positions in the DRR images. This relative shift is then applied to the three-dimensional (3D) isocenter from the treatment planning system. Therefore, each *cine* EPID image has a corresponding 3D shift in the treatment isocenter.

In the Eclipse treatment planning system (Varian Medical Systems, Inc.), each original planned beam is copied to the same number sub-beams as *cine* EPID images recorded for that beam. The sub-beams have the same geometry as the original planned beam; only the monitor units (MUs) will be different. The original number of MUs planned for the beam is distributed equally to the sub-beams. For example, if a treatment beam was originally planned to deliver 200 MU and 20 images were captured for that beam, then one would create 20 sub-beams each delivering 10 MU. Each sub-beam has a corresponding *cine* EPID image and, therefore, a corresponding isocenter shift associated with it, which is input manually. A plan consisting of six original treatment beams may have up to 200 sub-beams for calculating the delivered dose. The sub-beams are summed in the treatment planning system to find the daily delivered dose. The dose estimation for each fraction is summed to arrive at the total delivered 3D dose distribution.

## II.C. Convergent radiotherapy

An initial investigation of the concept of convergent radiation therapy has been performed using the clinical data from patient 4. As described in the previous publication, patient 4 (patient C in the previous publication) was positioned poorly on the first day of a three-fraction treatment. The *cine* EPID images of the implanted markers revealed a systematic

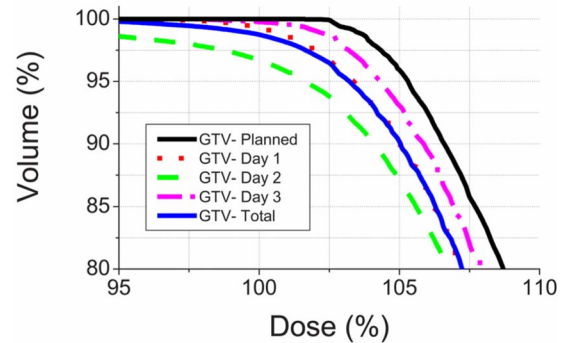


FIG. 1. For patient 1, DVH comparisons between delivered and planned dose for three fractions and the cumulative.

error of approximately 1.5 cm in the inferior direction. This resulted in an under-dosing or “cold region” in the most superior portion of the GTV. Although the shift was accounted for in subsequent fractions, the total delivered distribution still revealed an under-dosing of the GTV. Although the coverage on days 2 and 3 was excellent, the total prescription could not be reached.

Based on the delivered dose from the first fraction, two corrective strategies were investigated to achieve the prescribed coverage when all three fractions are combined. In Eclipse, a separate structure was defined based on the portion of the GTV that received less than 100% of the prescribed dose in the first fraction. New subfields were added to the plan to give a boost to the new structure. In corrective strategy No. 1 (CS1), a new plan is created for the second fraction only, and then the original plan is delivered for the third fraction. In corrective strategy No. 2 (CS2), a corrected plan is delivered on both of the remaining treatment days. Using the *cine* EPID data, both strategies were assessed by calculating the dose that would have been delivered.

## III. RESULTS

The exit radiation was collected for four patients during their external beam radiotherapy treatments. The delivered dose was reconstructed by comparing the fiducial locations in each *cine* EPID image to the reference positions in the corresponding DRR. The results for these patients are shown as dose-volume histograms (DVHs) of the planned and delivered doses.

For Patient 1, the target exhibited a drift towards the inferior, totaling 1 cm, during the second fraction. The dosimetric consequences of this movement can be quantified by the procedure above. It was found that, on this day, 97% of the GTV received 100% of the prescribed dose. The other fractions had better coverage, as indicated by their respective DVHs (see Fig. 1). From the sum of all three fractions, 99% of the GTV received 100% of the prescribed dose. The dosimetric effect of the unexpected target drift on day two was somewhat mitigated by the better target coverage on the other days of treatment.

Excellent target coverage was achieved for Patient 2 on each of the five days of treatment. In the cumulative DVH,

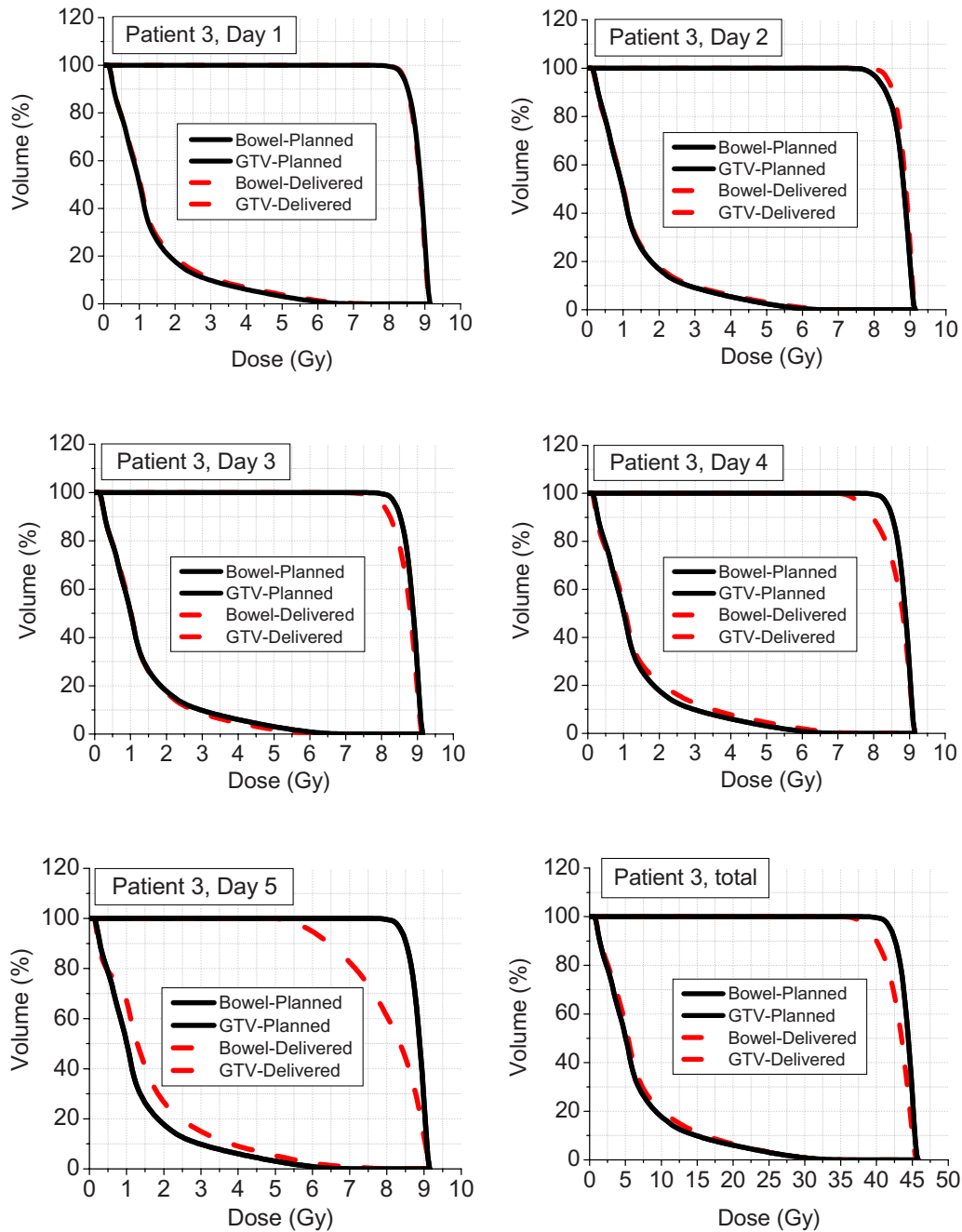


FIG. 2. For patient 3, DVH comparisons between delivered and planned dose for three fractions and the cumulative.

100% of the GTV receives 105% of the prescribed dose, as planned (not shown). This indicates an excellent setup and minimal residual motion for each treatment fraction.

For Patient 3, the target lay just posterior to a loop of bowel, necessitating a steep falloff of dose in that direction. For this patient, total dose (45 Gy) was prescribed to a point inside the GTV. The intention was to cover 100% of the GTV with 40 Gy (8 Gy per fraction). The target was well covered in the first four fractions, however a significant setup error led to an under-dosing on the final day of treatment (see Fig. 2). On this day, 100% of the GTV received a minimum of 5 Gy. The portion of bowel nearby received slightly more dose during this fraction than planned with a maximum of

~7.3 Gy (delivered) versus 7 Gy (planned). The cumulative delivered DVH shows reasonable tumor coverage with 100% of the tumor receiving ~36.5 Gy. The total mean GTV dose was 43.0 Gy, delivered, and 44.2 Gy, planned. The cumulative dose delivered to the adjacent bowel was only slightly higher than planned (mean: 7.2 Gy delivered, 6.7 Gy planned), with the same maximum dose (37.7 Gy) as planned.

There was a large error in the setup on the first day of treatment for Patient 4. This error was quantified with the *cine* EPID images and then an appropriate shift was recommended for the following two days of treatment. On day 1, 90% of the GTV received 100% of the prescription dose (see

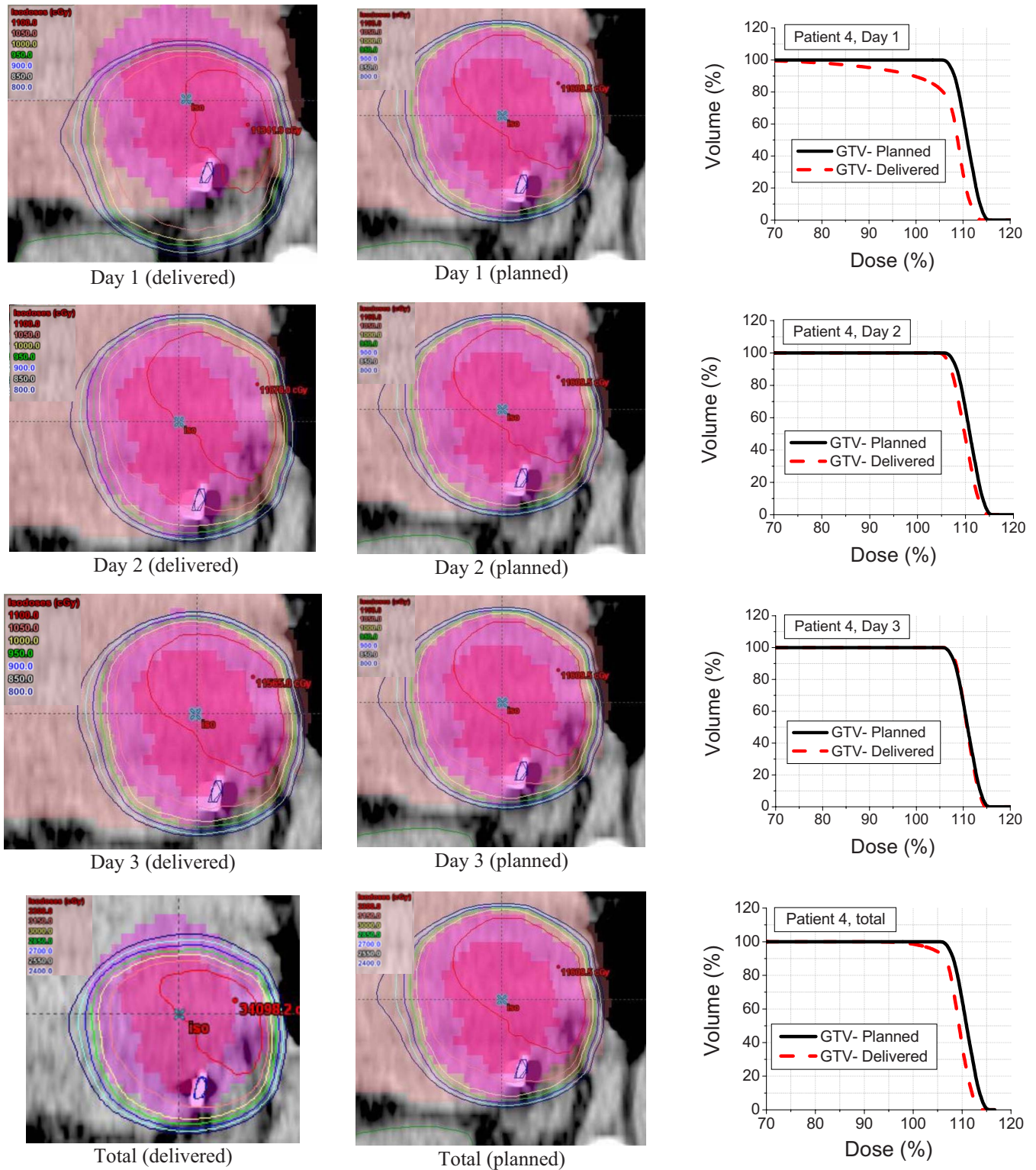


Fig. 3. For patient 4, (left) isodose distributions for the three fractions and the cumulative, (center) the planned isodose distributions, and (right) DVH comparisons between delivered and planned dose for three fractions and the cumulative.

Fig. 3). The superior portion of the GTV was colder than planned. A minimum of 69% of the prescribed dose was delivered here. On days 2 and 3, the GTV was well covered and the delivered dose closely follows the planned dose for those fractions. The cumulative DVH for the entire treatment shows that 98% of the GTV received 100% of the prescribed

dose. This data can also be shown as isodose curves on the planning CT (see Fig. 3).

The results of the two corrective strategies for Patient 4 are shown in Fig. 4. Both strategies provide better dosimetric coverage of the GTV compared to the delivered (uncorrected) treatment. In the DVHs, the differences between the

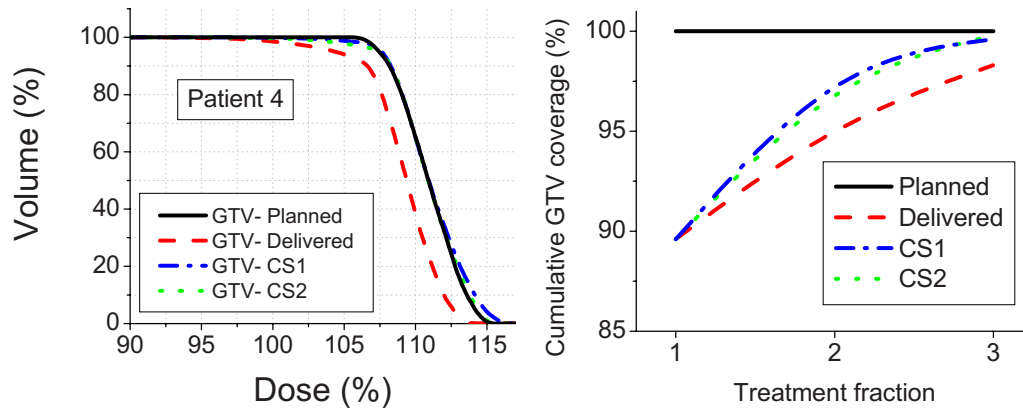


FIG. 4. Left: Comparison of the two corrective strategies (blue and green) with the planned (black) and delivered (red). Right: Using either of the two corrective strategies, the dose converges on what was planned.

two strategies are minimal. Both show increased hot spots within the target due to the residual target motion, the first day's dose gradient across the "boost" area and the concavity of the inferior portion of this new structure. With either strategy (CS1 or CS2), the delivered dose could have been estimated after the second day of treatment and if additional errors had been found, a new plan could have been made for the final day of treatment. The plot on the right of Fig. 4 shows how, with either of the corrective strategies, the delivered dose converges with the planned dose.

#### IV. DISCUSSION

A method for calculating the delivered dose using beam's-eye-view imaging has been presented. The data acquisition is simple to perform but the analysis must be done off-line, with an in-house developed program. Currently, it takes roughly 8 h to derive a delivered dose distribution for each fraction. A new automatic seed detection algorithm will shorten this to 5 h; an automatic method is being developed to feed the seed location information back into the treatment planning system to decrease the analysis time further. When these improvements are in place, delivered dose DVHs and isodose curves will be able to be generated very quickly after each treatment fraction. Our goal is to build a robust solution for calculating the delivered dose quickly, with a minimum amount of human interaction. We envision a function whereby the daily position information from each beam's-eye-view imaging session is transferred directly from PortalVision to Eclipse (without the time-consuming exporting) and cumulative dose distributions calculated. Depending on the computational speed, the distributions and corresponding DVHs would be available for on-line or off-line review. Calculation of the 3D delivered dose distribution would allow the physicist and/or clinician to perform daily or weekly off-line reviews of the dose coverage as the treatment progresses. If systematic errors are seen or the target coverage or dose to critical structures is not as desired, a new treatment plan could be created including, in the dose calculations, the fractions that have already been delivered.

Although the data acquisition does not interrupt the normal treatment flow, it has been found that cine EPID acquisition is incompatible with dynamic wedging. The acquisition is stopped when the jaw begins to move across the field, so images can only be acquired for the open portion. Therefore the treatment planners are asked to use physical wedges when wedging is necessary. Physical wedges do not obscure the visualization of the seeds in the EPID images.

The assumption that the shift only occurs in the imaging plane through isocenter is a source of error. One would expect intra-fractional movements of the target in the lateral and anterior-posterior directions to never exceed 2 cm. In the worst-case scenario, this maximum error could occur in the unresolved direction (i.e., parallel to the beam). A 2 cm error in depth corresponds to a dosimetric error of approximately 10% (depending on the depth), however, this error would be somewhat negated by any other beam at a near-opposing angle. Using the treatment parameters from patient 2 (9 coplanar angles), it was found that the dosimetric error at isocenter would be largest for a 2 cm shift in the right lateral direction ( $<4\%$ ). The dosimetric error from a 1 cm shift in any direction is never greater than 1.7%. For the patients studied, shifts in the lateral or anterior-posterior direction never exceed 0.5 cm.

So far, the data taking has concentrated on 3D conformal (non-IMRT) delivery. It is unclear how best to extend the BEV imaging modality to IMRT delivery in the future, or whether it is even necessary. Obviously problems will arise due to the small openings in each IMRT segment. Not all of the implanted markers (if any) will be visible in all of the recorded images. However, it may be found that the margin reduction allowable with the cine EPID technique provides better dose distributions than an IMRT delivery with no in-treatment verification, obviating the need for IMRT, in some cases. This will be the subject of a future study.

Although the method has been presented for liver SBRT treatments, it may be applied to other sites where implanting fiducials is clinically feasible. In the case of lung tumor irradiation, many clinics do not implant fiducials due to the risk of pneumothorax.<sup>12-16</sup> Methods are currently under develop-

ment for finding the relative shifts between the scenes in the cine EPID images and the DRR (or DRF—digitally reconstructed fluoroscopy) without the aid of implanted fiducials.<sup>17–20</sup> Once this relationship is determined, the delivered dose estimation algorithm can proceed as described above.

## V. CONCLUSION

The dose delivered to a patient can be estimated using beam's-eye-view *cine* EPID images acquired during radiotherapy treatment. The data acquisition does not disrupt or add any additional time to the treatment. The target position analysis is performed off-line and then the delivered dose is estimated using the Eclipse treatment planning software. This technique could be useful for quality assurance, accurate planning of multiple radiotherapy courses, and clinical delivered dose response studies.

## ACKNOWLEDGMENTS

The authors wish to thank the therapists at the Brigham and Women's Hospital for their help with this study. This project was partially supported by grants from Varian Medical Systems, Inc. and the JCRT Foundation.

<sup>a)</sup>Author to whom correspondence should be addressed; electronic mail: rberbeco@iroc.harvard.edu

<sup>1</sup>C. W. Scarantino, D. M. Ruslander, C. J. Rini, G. G. Mann, H. T. Nagle, and R. D. Black, "An implantable radiation dosimeter for use in external beam radiation therapy," *Med. Phys.* **31**, 2658–2671 (2004).

<sup>2</sup>Y. Yang, E. Schreiber, T. F. Li, C. Wang, and L. Xing, "Evaluation of on-board kV cone beam CT (CBCT)-based dose calculation," *Phys. Med. Biol.* **52**, 685–705 (2007).

<sup>3</sup>L. McDermott, M. Wendling, J. Nijkamp, A. Mans, J. J. Sonke, B. Mijnheer, and M. van Herk, "3D in vivo dose verification of entire hypofractionated IMRT treatments using an EPID and cone-beam CT," *Radiother. Oncol.* **86**, 35–42 (2008).

<sup>4</sup>B. W. Raaymakers, A. J. E. Raaijmakers, A. Kotte, D. Jette, and J. J. W. Lagendijk, "Integrating a MRI scanner with a 6 MV radiotherapy accelerator: Dose deposition in a transverse magnetic field," *Phys. Med. Biol.* **49**, 4109–4118 (2004).

<sup>5</sup>J. Dempsey, B. Dionne, J. Fitzsimmons, A. Haghigat, J. Li, D. Low, S. Mutic, J. Palta, H. Romeijn, and G. Sjoden, "A real-time MRI guided

external beam radiotherapy delivery system," *Med. Phys.* **33**, 2254–54 (2006).

<sup>6</sup>S. Steciw, T. Stanescu, M. Carlone, and B. Fallone, "Magnetic shielding of a coupled MRI-Linac system," *Med. Phys.* **34**, 2623–23 (2007).

<sup>7</sup>D. W. Litzenberg, S. W. Hadley, N. Tyagi, J. M. Baiter, R. K. Ten Haken, and I. J. Chetty, "Synchronized dynamic dose reconstruction," *Med. Phys.* **34**, 91–102 (2007).

<sup>8</sup>W. Kilby and C. Savage, "The effect of the Varian amorphous silicon electronic portal imaging device on exit skin dose," *Phys. Med. Biol.* **48**, 3117–3128 (2003).

<sup>9</sup>R. I. Berbeco, T. Neicu, E. Rietzel, G. T. Chen, and S. B. Jiang, "A technique for respiratory-gated radiotherapy treatment verification with an EPID in cine mode," *Phys. Med. Biol.* **50**, 3669–3679 (2005).

<sup>10</sup>D. Yan, F. Vicini, J. Wong, and A. Martinez, "Adaptive radiation therapy," *Phys. Med. Biol.* **42**, 123–132 (1997).

<sup>11</sup>R. Berbeco, F. Hacker, D. Ionascu, and H. Mamon, "Clinical feasibility of using an EPID in cine mode for image-guided verification of SBRT," *Int. J. Radiat. Oncol., Biol., Phys.* **69**, 258–266 (2007).

<sup>12</sup>U. Topal and B. Ediz, "Transthoracic needle biopsy: Factors effecting risk of pneumothorax," *Eur. J. Radiol.* **48**, 263–267 (2003).

<sup>13</sup>P. R. Geraghty, S. T. Kee, G. McFarlane, M. K. Razavi, D. Y. Sze, and M. D. Dake, "CT-guided transthoracic needle aspiration biopsy of pulmonary nodules: Needle size and pneumothorax rate," *Radiology* **229**, 475–481 (2003).

<sup>14</sup>S. Arslan, A. Yilmaz, B. Bayramgurler, O. Uzman, E. Nver, and E. Akkaya, "CT-guided transthoracic fine needle aspiration of pulmonary lesions: Accuracy and complications in 294 patients," *Med. Sci. Monit* **8**, CR493–497 (2002).

<sup>15</sup>F. Laurent, V. Latrabe, B. Vergier, and P. Michel, "Percutaneous CT-guided biopsy of the lung: Comparison between aspiration and automated cutting needles using a coaxial technique," *Cardiovasc. Intervent Radiol.* **23**, 266–272 (2000).

<sup>16</sup>F. Laurent, V. Latrabe, B. Vergier, M. Montaudon, J. M. Vernejoux, and J. Dubrez, "CT-guided transthoracic needle biopsy of pulmonary nodules smaller than 20 mm: Results with an automated 20-gauge coaxial cutting needle," *Clin. Radiol.* **55**, 281–287 (2000).

<sup>17</sup>R. Berbeco, H. Mostafavi, G. C. Sharp, and S. B. Jiang, "Tumor Tracking in the Absence of Radiopaque Markers," XIVth ICCR 433–36 (2004).

<sup>18</sup>R. I. Berbeco, H. Mostafavi, G. C. Sharp, and S. B. Jiang, "Towards fluoroscopic respiratory gating for lung tumours without radiopaque markers," *Phys. Med. Biol.* **50**, 4481–4890 (2005).

<sup>19</sup>D. Ionascu, S. Park, J. Killoran, A. Allen, and R. Berbeco, "Marker-less intra-fraction position verification of lung tumors with an EPID in cine mode," *Med. Phys.* **34**, 2528 (2007).

<sup>20</sup>Q. Y. Xu, R. J. Hamilton, R. A. Schowengerdt, and S. B. Jiang, "A deformable lung tumor tracking method in fluoroscopic video using active shape models: A feasibility study," *Phys. Med. Biol.* **52**, 5277–5293 (2007).